STIFFNESS ASSESSMENT OF BOLTED BEAM-TO-TUBULAR COLUMN JOINTS THROUGH MODAL DATA

MIGUEL A. SERRANO-LOPEZ[1], MARTAGARCÍA-DIÉGUEZ[1], JOSEL.ZAPICO-VALLE[1], CARLOS LOPEZ-COLINA[1]and MIGUEL LOZANO[1]

[1]*Departmentof Construction and Manufacturing Engineering, University of Oviedo, Campus de Gijón, 33203, Gijón-Spain.*
E-mail: serrano@uniovi.es

Although beam-to-tubular column joints are mostly welded instead of bolted because the difficulty to access to the inside of tubes, the use of threaded studs welded to the tube front face of rectangular hollow sections could avoid this problem and allows removable joints to be used. An important issue of these connections is the characterization of their rotational stiffness. A research on bolted I beam-to-tubular column joints using welded threaded studs, which proposes a new methodology to obtain the joint stiffness from modal data, is presented in this paper. The studied joints include angle cleats connected to the beam flanges with standard bolts and to the column face with welded threaded studs. A simplified finite element model comprising beam elements has been developed to reproduce the dynamic behavior of this kind of connections. The model is updated by minimizing the discrepancies between the analytical and experimental natural frequencies. The experimental frequencies were obtained through modal impact tests. The initial rotational stiffness, which is an essential parameter to characterize semi-rigid joints, can be easily obtained from the updated model. On the experimental side, the proposed procedure just needs a portable analyzer and an accelerometer. The goodness of the model has been validated with experimental monotonic tests and results are really promising.

Keywords: Modal identification, Model updating, Rotational stiffness, Bolted connections, Rectangular hollow sections.

1 Introduction

It is known that hollow steel sections are a good alternative to H-sections in columns due to several advantages regarding the mechanical behavior, higher fire resistance or just to improve the aesthetics Edkhout (2011), Wardenier et al. (2010) and Kurobane et al. (2004).A good option in ordinary buildings is to combine open section beams that present high flexural resistance with tubular columns with high efficiency acting as beam-column members. Due to the inability to access to the inside of tubes, these beam-to-tubular column joints are typically welded, welding the entire beam open profile or sometimes welding only the beam flanges, Serrano et al. (2019). The available bolted solutions based on using blind bolts are expensive, nevertheless a bolted joint based on threaded studs that are easily welded to the tube walls could be an interesting alternative Serrano et al. (2019). An important issue regarding connections is their characterization in terms of rotational stiffness to be considered in the structural analysis, Eurocode 3-1.8 (2005). Traditionally, the initial rotational stiffness is obtained through static tests based on the moment-rotation curve plotted from the recorded data. An alternative

Proceedings of the 17th International Symposium on Tubular Structures.
Editors: X.D. Qian and Y.S. Choo

Published by Research Publishing, Singapore.
ISBN: 978-981-11-0745-0; doi:10.3850/978-981-11-0745-0_015-cd

approach could be based on modal data of full-scale joints, Türker(2009) andZapico-Valle et al.(2012).

In this paper, a non-destructive procedure to estimate the initial rotational stiffness of bolted beam-to-tubular column joints through modal data has been developed. The modal data were obtained from impact tests carried out on nine different full-scale specimens of this kind of joint. The experimental data are used to calibrate a finite element model comprising beam elements through a model updating procedure. The updating is posed as the minimization of the discrepancies between the experimental and analytical natural frequencies. The initial rotation stiffness is obtained from the updated model. Finally, the static and dynamic estimations of the initial stiffness are compared.

2 Experimental part

2.1 *Descriptions of the specimens*

Nine different configurations of bolted beam-to-tubular column joints have been considered in this paper. Each configuration combines open section I beams (HEB200 or IPE300) with tubular columns (SHS200 or RHS200×150). Six different columns were used varying wall thicknesses (6, 8 and 10 mm). These configurations are common in buildings with ordinary loads. The configurations are summarized in Table 1 along with identification code from SMS1 to SMS9.

Table 1. Sections of beam-column joints.

Specimen	Column	Beam
SMS1	SHS200×6	HEB200
SMS2	SHS200×8	HEB200
SMS3	SHS200×10	HEB200
SMS4	SHS200×6	IPE300
SMS5	SHS200×8	IPE300
SMS6	SHS200×10	IPE300
SMS7	RHS200×150×6	IPE300
SMS8	RHS200×150×8	IPE300
SMS9	RHS200×150×10	IPE300

Each specimen included two non-symmetrical angle cleats 120x80x10 bolted to the column face and the beam flanges. The long leg of the angle cleat was bolted with four ordinary bolts to the flanges of the beam. The short leg of the angle cleats was connected to the column through a pair of welded threaded studs. The length of angle cleats was equal to the corresponding beam flange width. That means 200mm for the HEB and 150mm for the IPE beams. S275 grade of steel were used in tubes, beams and angles. Standard bolts M16 grade 10.9 were used to connect the long leg of the angles to the beam flanges by means of a calibrated torque wrench of 250 Nm. The threaded studs were M16 grade K800×40, the total length of the stud being 40 mm. The studs were welded to the tube front face without any specialized workforce using a portable welding machine INOTOP 1704 and welded pistol KE30. After welding and positioning the pieces, the nuts on the studs were tightened by means of a calibrated torque wrench of 190 Nm.

2.2 *Dynamic tests*

The physical models were dynamically tested under free boundary conditions. For this purpose, each specimen was suspended in the air by means of a bridge crane connected to the specimen through a sling, as shown in figure 1. Impact tests were performed with an ordinary hammer and

only one accelerometer (100 mV/g) located at different positions. A CSI 2120 portable analyzer was used to process the signal and to obtain the FRF and its corresponding natural frequencies. In a preliminary stage, several accelerometer and impact positions were tried in order to extract as much information as possible. The first mode was easily obtained impacting horizontally on the beam end and locating the accelerometer vertically on the tube (Figure 1-left). And the third mode was obtained locating the accelerometer horizontally in the beam (Figure 1-right) and impacting in the same point. Both frequencies were accurately obtained in all the specimens. The obtained first and third experimental frequencies, respectively labelled as f_1^e and f_3^e, for each specimen are presented in Table 2.

Table 2. Experimental frequencies f_1^e and f_3^e from impact tests.

Specimen	f_1^e [Hz]	f_3^e [Hz]
SMS1	168	628
SMS2	226	620
SMS3	207	611
SMS4	186	1057
SMS5	253	1058
SMS6	302	1082
SMS7	302	754
SMS8	332	1103
SMS9	416	1024

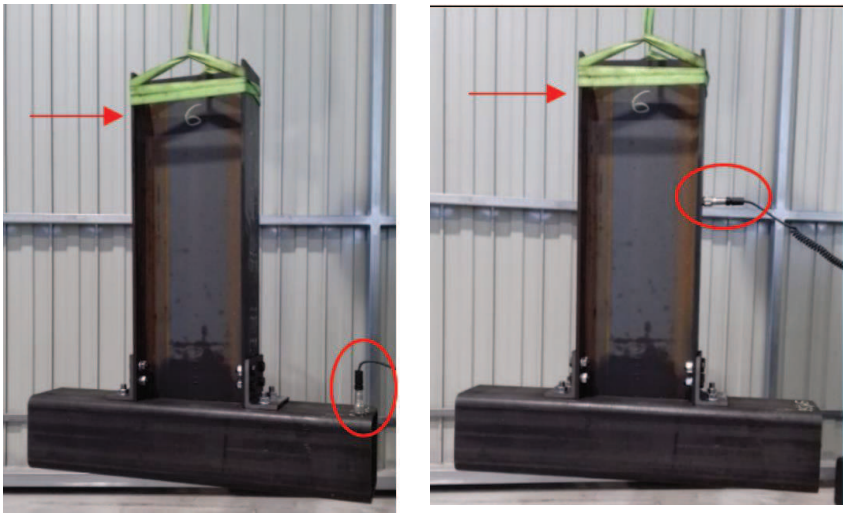

Figure 1.Dynamic test set-up. Left: First mode. Right: Third mode.

2.3 *Static tests*

The nine beam-column joints (SMS1 to SMS9) described in the above section 2.1 were tested under displacement control and monotonic loading at a speed of 4 mm/min. The load was applied by means of a hydraulic actuator Ibertest GIB 500-MD2W attached to a multi-positional reaction frame. This actuator is able to reach a maximum load of 500 kN and a maximum displacement of 200 mm. A vertical displacement was applied on top of the free end of the beam as can be seen in figure 2. To prevent any horizontal movement of the joint, the top and bottom

parts of the column were tied to the frame by means of 20 mm rods that were firmly tightened. A DIC (digital image correlation) equipment Aramis model 5M was used during the tests. This was synchronized with the jack, allowing the applied force to be recorded and the deformations over the specimen surfaces to be measured by means of high resolution 3D images at the same time. The beam rotation was measured with the DIC and the corresponding bending moment at the connection section of the beam was calculated in a continuous way. This allowed the moment rotation curves to be plotted and the experimental initial rotational stiffness of the joints to be extracted from them. Figure 2 shows the general set up for a pair of joints during their tests (SMS2 on the left and SMS8 on the right).

Figure 2. General set-up of static tests

3 Analytical part

3.1 *General approach*

The analytical modelling of the specimens is essential to succeed in calibrating the initial rotational stiffness of the joint. The analytical model should contain the features of the physical one. The main particularity of the studied joints is that the beam-to-column connection is localized at the angles, which are placed at the edges of the beam end. This gives rise to an additional shear flexibility of the joint that affects significantly the dynamic behavior of the specimens and therefore should be taking into account. It is also hypothesized that the transmission of forces between beam and column is concentrated at the studs. The further modelling will be based on these assumptions.

3.2 *Finite element modelling*

A finite element model composed by beam elements is used to characterize the in-plane dynamic behavior of the specimens (Figure 3-left). The sling is modelled through a bar element, E, fixed at an end (node 25) and pinned to the beam end (node 22). Both the beam and the column are modelled as Timoshenko beams corresponding to their axes, A and B, which are split into eight

and twelve elements, respectively (nodes 14 to 22 and 1 to 13). The geometrical properties adopted for the elements are presented in Table 3.

Table 3. Nominal properties of the cross-sections.

Section	Area $[m^2]$	Equivalent shear area $[m^2]$	Second moment of area $[m^4]$
SHS200×6	$4.56\ 10^{-3}$	$2.40\ 10^{-3}$	$2.833\ 10^{-5}$
SHS200×8	$5.92\ 10^{-3}$	$3.20\ 10^{-3}$	$3.566\ 10^{-5}$
SHS200×10	$7.26\ 10^{-3}$	$4.00\ 10^{-3}$	$4.251\ 10^{-5}$
RHS200×150.6	$3.96\ 10^{-3}$	$2.40\ 10^{-3}$	$2.268\ 10^{-5}$
RHS200×150.8	$5.12\ 10^{-3}$	$3.20\ 10^{-3}$	$2.829\ 10^{-5}$
RHS200×150.10	$6.26\ 10^{-3}$	$4.00\ 10^{-3}$	$3.348\ 10^{-5}$
HEB200	$7.81\ 10^{-3}$	$2.48\ 10^{-3}$	$5.696\ 10^{-5}$
IPE300	$5.38\ 10^{-3}$	$2.57\ 10^{-3}$	$8.360\ 10^{-5}$

Two additional elements, C and D, are used to model the joint itself. Elements C (nodes 14, 23 and 14, 24) are rigidly connected to the beam end (node 14). These are mass-less and rigid elements. The rigidity is achieved by choosing an area and second moment of area of the cross-section several orders of magnitude higher than those of the sections (Table 4). Nodes 23 and 24 are aligned with the stud axes. Elements D (node 5, 23 and 9, 24) are rigidly connected to the column (nodes 5 and 9) and pinned to the ends of elements C (nodes 23 and 24). These elements coincided with the stud axes and are modelled as mass-less Bernoulli beams. The area and moment of area of the cross-sections of these elements, A_D and I_D, provide respectively the rotation and translation flexibility to the joint. They are chosen as the parameters to be updated. Young's modulus and Poisson's coefficient were set respectively equal to $2.1\ 10^{11}$ Pa and 0.3 for all the elements.

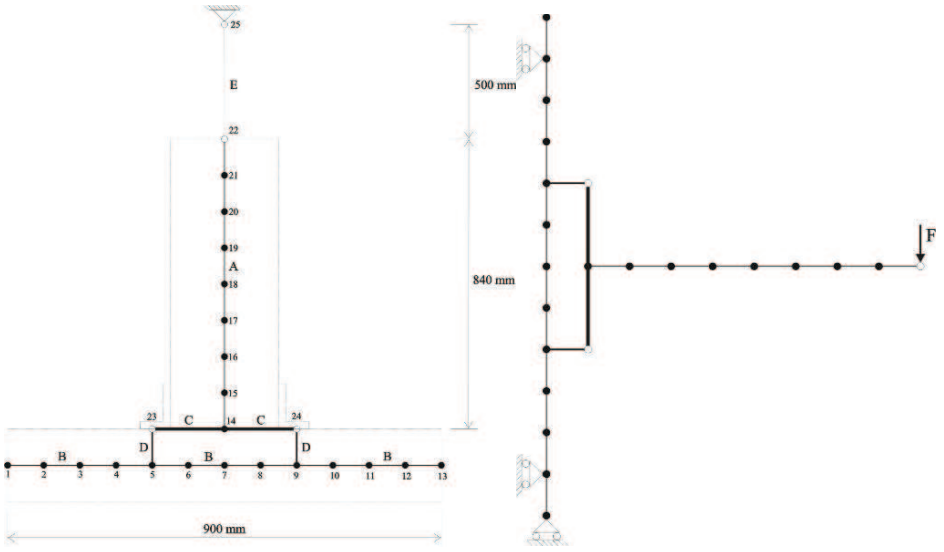

Figure 3. Finite element model scheme along with section types and main dimensions. Left: Dynamic model. Right: Static model.

Table 4. Mechanical properties of the elements.

Element	Area $[m^2]$	Second moment of area $[m^4]$	Density $[kg/m^3]$
A	Corresponding beam	Corresponding beam	7850
B	Corresponding column	Corresponding column	7850
C	10	10	0
D	A_D	I_D	0
E	$7 \cdot 10^{-7}$	0	0

3.3 *Model updating*

The updating of parameters A_D and I_D is posed as the minimization of an error function that accounts for the discrepancies between the experimental natural frequencies, $f_j^{(e)}$, and those predicted by the model, $f_j^{(a)}$. Modes 1 and 3, which exhibit a remarkable rotation and translation of the joint (Figure 4), are chosen for the updating. A quadratic error function, Eq.(1),is selected to quantify the discrepancies

$$\varepsilon_f = \frac{1}{2}\left[\left(\frac{f_1^{(a)} - f_1^{(e)}}{f_1^{(e)}}\right)^2 + \left(\frac{f_3^{(a)} - f_3^{(e)}}{f_3^{(e)}}\right)^2\right] \tag{1}$$

The minimization is carried out through an adaptive stochastic algorithm described in Zapico-Valle et al. (2010). Results of the updating are presented in Table 5. In all the studied cases the final fitting error was lower than 10^{-20}.

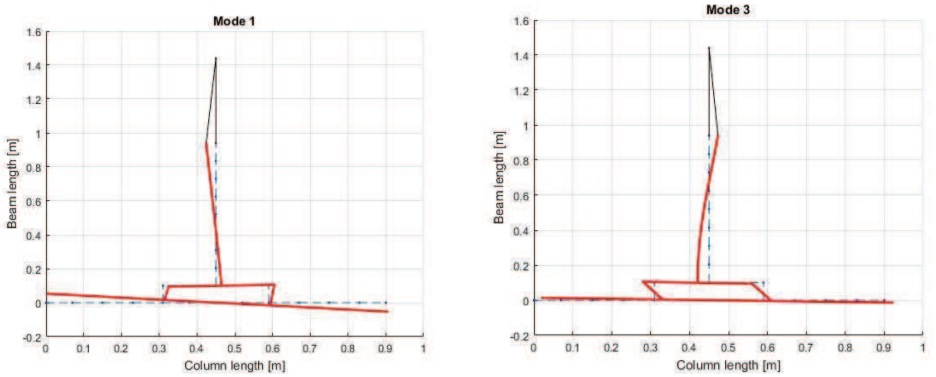

Figure 4. Modes for updating purpose. Discontinuous line: Initial position. Bold line: Mode shape.

Table 5. Updated parameters for each joint.

Specimen	A_D $[m^2]$	I_D $[m^4]$
SMS1	$2.144\ 10^{-5}$	$1.644\ 10^{-7}$
SMS2	$5.098\ 10^{-5}$	$1.777\ 10^{-7}$
SMS3	$4.932\ 10^{-5}$	$1.846\ 10^{-7}$
SMS4	$1.292\ 10^{-5}$	$4.440\ 10^{-7}$
SMS5	$3.059\ 10^{-5}$	$4.883\ 10^{-7}$

SMS6	$5.396\ 10^{-5}$	$5.552\ 10^{-7}$
SMS7	$3.309\ 10^{-5}$	$1.825\ 10^{-7}$
SMS8	$5.056\ 10^{-5}$	$5.235\ 10^{-7}$
SMS9	$10.76\ 10^{-5}$	$4.509\ 10^{-7}$

3.4 *Initial stiffness*

The initial rotational stiffness is estimated through two different approaches. One is based on the moment-rotation data coming from the monotonic static tests and another relies on the updated finite element models. In the static approach, the first 100 moment-rotation points identified from the experiments are fit to a first-order polynomial by the least squares method (Figure 5). The first coefficient of the polynomial is chosen as an estimation of the initial stiffness,S_{ini}^{s}. The range of the selected points corresponds to a maximum rotation around $5 \cdot 10^{-3}\ rad$.

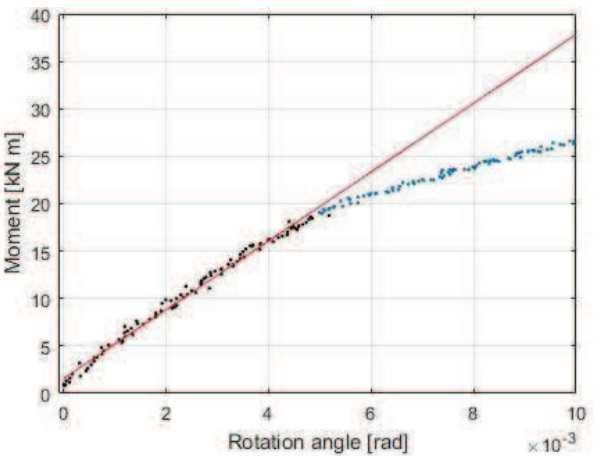

Figure 5. Moment-rotation curve for joint SMS7. Dots: experimental data. Line: Linear fit.

In the dynamic approach, the updated finite element model is modified to reproduce the boundary conditions of the static test (Figure 3-right). The sling is remove from the model and nodes 2, 12 and 13 are fixed by pinned supports. Moreover, a force, F, is applied at node 22. The rotation, θ, of node 14 due to a unitary force, $F = 1$, is computed through this model and from the results the initial stiffness is estimated by Eq. (2),where 0.84 m is the arm of the force.

$$S_{ini}^{d} = \frac{0.84}{\theta} \tag{2}$$

Results of both dynamic and static approaches are presented in Table 6 along with the discrepancies,ε_s, of the dynamic results relative to the static results. In six out of nine cases the dynamic results are higher than the static ones, the discrepancies being in average around 10%. An explanation of these outcomes could be that the displacement during the dynamic tests are very low, while those of the selected points in the static tests are higher giving rise to softening effects. Results are nevertheless very close from a practical point of view allowing the propose method to be validated.

Table 6. Initial stiffness comparative between dynamic, S_{ini}^{d}, and static, S_{ini}^{s}, estimation.

Joint	S_{ini}^{d} [Nm/rad]	S_{ini}^{s} [Nm/rad]	ε_S [%]
SMS1	$1.696\ 10^6$	$1.832\ 10^6$	-7.44
SMS2	$3.878\ 10^6$	$3.019\ 10^6$	28.46
SMS3	$3.792\ 10^6$	$3.755\ 10^6$	0.99
SMS4	$1.905\ 10^6$	$1.967\ 10^6$	-3.15
SMS5	$4.391\ 10^6$	$4.416\ 10^6$	-0.57
SMS6	$7.511\ 10^6$	$6.036\ 10^6$	24.45
SMS7	$4.675\ 10^6$	$3.626\ 10^6$	28.93
SMS8	$6.999\ 10^6$	$6.197\ 10^6$	12.93
SMS9	$13.810\ 10^6$	$12.521\ 10^6$	10.29

4 Conclusions

Static and dynamic tests have been carried out on a set of nine full-scale bolted beam-to-tubular column joints using threaded studs welded to the tube. Angle cleats bolted to the beam flanges connect them to the tube by means of the studs. The aim of this paper was to obtain the initial rotational stiffness of the joint by a different and easier procedure than the traditional one. The procedure relies on a finite element model compose of beam elements. The model includes the main features of these joints and is calibrated against modal data. The procedure has been applied to nine different specimens of this joint. The comparison of results with those obtained from static test on the same specimens allows the procedure to be validated. The proposal is of practical application because it does not need the use of expensive facilities.

Acknowledgments

The authors would like to acknowledge the Spanish Ministry of Economy and Competitiveness for their financial support under Project BIA2017-83467-P and the CIDECT for their support under project 5CF.

References

CEN, EN-1993-1-8:2005. *Eurocode 3:Design of steel structures. Part 1-8: Design of Joints*. European Committee for Standardization. 2005.

Edkhout, M.,*Tubular Structures in Architecture*, CIDECT, Geneva and TU Delft, 2011.

Kurobane, Y., Packer, J.A., Wardenier, J., Yeomans, N. *Design guide for structural hollow sections columnconnections*. CIDECT, TÜV-Verlag GmbH, Köln, 2004.

Serrano, M. A., López-Colina, C., Wang, Y.C., Lozano, M. and Gayarre, F.L., Comparative behaviour of 'I beam- RHS column' joints with and without web weld, *J. Constr. Steel Res.*, 159, 330-340, 2019.

Serrano, M. A., López-Colina, C., Wang, Y.C., Lozano, M. and Gayarre, F.L., *I beam-RHS column joints with welded studs,* Proceedings of the 9thIntnl. Conf. on Steel and Alum. Struct., Badford, July 3-5, 2019.

Türker, T., Kartal, M.E., Bayraktar, A., Muvafik, M., Assessment of semi-rigid connections in steel structures by modal testing,*Journal of Constructional Steel Research* 65(7), 1538-1547, 2009.

Wardenier, J., Packer, J.A., Zhao, X.L. and van der Vegte, G.J.,*Hollow sections in structural applications*. 2nded. CIDECT, Geneva, 2010.

Zapico-Valle, J.L., Abad-Blasco, J., González-Martínez, M.P., Franco-Gimeno, J.M. and García-Diéguez, M.,Modelling and calibration of a beam-column joint based on modal data,*Computers and Structures* 108-109, 31-41, 2012.

Zapico-Valle, J.L., Alonso-Camblor, R., González-Martínez, M.P. and García-Diéguez, M.,A new method for finite element model updating in structural dynamics,*Mechanical Systems and Signal Processing* 24(7), 2137-2159, 2010.